INTERNATIONAL JOURNAL FOR NUMERICAL METHODS IN FLUIDS
Int. J. Numer. Meth. Fluids 2005; **47**:1077–1083
Published online 17 January 2005 in Wiley InterScience (www.interscience.wiley.com). DOI: 10.1002/fld.860

A moving mesh finite element algorithm for fluid flow problems with moving boundaries

M. J. Baines[1], M. E. Hubbard[2,*,†] and P. K. Jimack[2]

[1]*Department of Mathematics, University of Reading, WhiteKnights, PO Box 220, Berkshire, RG6 6AX, U.K.*
[2]*School of Computing, The University of Leeds, LS2 9JT Leeds, U.K.*

SUMMARY

A moving mesh finite element method is proposed for the adaptive solution of second- and fourth-order moving boundary problems which exhibit scale invariance. The equations for the mesh movement are based upon the local application of a scale-invariant conservation principle incorporating a monitor function and have been successfully applied to problems in both one and two space dimensions. Examples are provided to show the performance of the proposed algorithm using a monitor function based upon arc-length. Copyright © 2005 John Wiley & Sons, Ltd.

KEY WORDS: moving boundaries; moving meshes; finite element method; scale invariance

1. INTRODUCTION

Moving meshes have proved to be a valuable tool in Computational Fluid Dynamics, having been successfully applied in many different contexts, ranging from phase change and blow-up problems to hyperbolic conservation laws and more general classes of time-dependent flow. In this paper a moving mesh finite element method is presented for the solution of a class of scale-invariant partial differential equations (PDEs) with moving boundaries. Although no analysis is presented, the numerical experiments suggest that the approach exhibits similar stability properties to standard, fixed mesh, finite element methods.

The moving mesh approach has been rekindled by recent interest in geometric integration and scale invariance, which treats independent and dependent variables alike [1]. In this paper, the mesh equations are based on the principle of conserving the integral of a scale invariant monitor function in time within each patch of finite elements. An additional constraint is required to specify the mesh velocity uniquely, this being carried out through

*Correspondence to: M. E. Hubbard, School of Computing, The University of Leeds, LS2 9JT Leeds, U.K.
†E-mail: meh@comp.leeds.ac.uk

Contract/grant sponsor: EPSRC; contract/grant number: GR/R94862/01

Received 27 April 2004
Revised 2 August 2004
Accepted 9 August 2004

a mesh velocity potential in the manner of Reference [2]. Unlike most approaches to moving boundary problems, the approximation procedure uses the PDE to obtain the mesh velocities: based upon an approach that has already been successfully applied to a range of moving boundary problems in one and two space dimensions using the dependent variable as monitor function [3].

1.1. Scale invariance

Scaling is a natural property of models of physical systems due to their independence of physical units [4]. For a scale invariant problem there exist indices β and γ such that the scaling

$$t = \lambda \hat{t}, \quad \mathbf{x} = \lambda^{\beta} \hat{\mathbf{x}}, \quad u = \lambda^{\gamma} \hat{u} \tag{1}$$

leaves the PDE

$$u_t = Lu \tag{2}$$

(where Lu is a purely spatial operator on an evolving domain $\Omega(t)$) and appropriate boundary conditions invariant. For example, in the case of the porous medium equation (PME) in d dimensions, which represents isentropic gas flow through porous media,

$$u_t = \nabla \cdot (u^n \nabla u) \quad \text{subject to } u|_{\partial\Omega} = 0 \tag{3}$$

it can be shown that $\beta = 1/(nd+2)$ and $\gamma = -d/(nd+2)$, while for the fourth-order equation

$$u_t + \nabla \cdot (u^n \nabla \nabla^2 u) = 0 \quad \text{subject to } u|_{\partial\Omega} = \left.\frac{\partial u}{\partial n}\right|_{\partial\Omega} = 0 \tag{4}$$

$\beta = 1/(nd+4)$ and $\gamma = -d/(nd+4)$. A range of applications of this equation can be found in Reference [5] (and references therein). For both these problems there exist known self-similar solutions, [5, 6], which are ideal for comparison with the results obtained by numerical schemes.

1.2. Monitor functions and conservation

Given an initial condition for (2), a set of test functions w_i, and a non-negative, solution-dependent monitor function $m(u, \nabla u)$, then one may define $k_i \in [0, 1]$ such that

$$\int_{\Omega} w_i m(u, \nabla u)\, \mathrm{d}\Omega = k_i \int_{\Omega} m(u, \nabla u)\, \mathrm{d}\Omega = c_i \text{ say} \tag{5}$$

If the test functions form a partition of unity then $\sum_i k_i = 1$. Furthermore, conservation of (5), as the solution u and domain $\Omega(t)$ evolve in time, may be used as the guiding principle for a mesh movement algorithm (as in Reference [3] with $m(u, \nabla u) \equiv u$). For a scale invariant problem (5) may be modified to become

$$\int_{\Omega(t)} w_i \tilde{m}(t, u, \nabla u)\, \mathrm{d}\Omega = c_i \tag{6}$$

where the w_i are scale invariant and $\tilde{m}$ is given by

$$\tilde{m}(t,u,\nabla u)=t^{-d\beta}m(t^{-\gamma}u,t^{-\gamma+\beta}\nabla u) \tag{7}$$

Note that $\tilde{m}=m$ at $t=1$ (which, without loss of generality, is taken to be the initial time throughout this paper) and that, as a result of scale invariance, the c_i are now independent of t. We shall refer to Equation (6) as the conservation principle. This equation suggests the existence of a mapping $\mathbf{x}(t)$ for which scale invariance is sustained for all $t\geqslant 1$. We next derive the velocity $\dot{\mathbf{x}}(t)$ explicitly by differentiating (6) with respect to t.

1.3. The velocity $\dot{\mathbf{x}}(t)$

Using Leibniz's rule (aka the Reynolds Transport Theorem) and assuming that $\partial w_i/\partial t+\dot{\mathbf{x}}\cdot\nabla w_i=0$ (i.e. the test function w_i is advected with velocity $\dot{\mathbf{x}}$), we obtain from (6)

$$\begin{aligned}0&=\frac{\partial}{\partial t}\int_{\Omega(t)}w_i\tilde{m}(t,u,\nabla u)\,\mathrm{d}\Omega=\int_{\Omega(t)}\left(\frac{\mathrm{d}}{\mathrm{d}t}(w_i\tilde{m})+\nabla\cdot(w_i\tilde{m}\dot{\mathbf{x}})\right)\mathrm{d}\Omega\\&=\int_{\Omega(t)}w_i\left(\frac{\partial\tilde{m}}{\partial t}+\left(\frac{\partial\tilde{m}}{\partial u}+\frac{\partial\tilde{m}}{\partial\nabla u}\cdot\nabla\right)\frac{\partial u}{\partial t}+\nabla\cdot(\tilde{m}\dot{\mathbf{x}})\right)\mathrm{d}\Omega\end{aligned} \tag{8}$$

If we now substitute for $\partial u/\partial t$ from the PDE, (2), this becomes an equation for $\dot{\mathbf{x}}$. By itself this is insufficient to determine $\dot{\mathbf{x}}$ uniquely in more than one space dimension. However, by the Helmholtz Decomposition Theorem uniqueness may be obtained by additionally specifying $\operatorname{curl}\dot{\mathbf{x}}$ and a suitable boundary condition. By writing $\operatorname{curl}\dot{\mathbf{x}}=\operatorname{curl}\mathbf{v}$, where $\mathbf{v}$ is prescribed, it follows that there exists a potential function ϕ such that $\dot{\mathbf{x}}=\mathbf{v}+\nabla\phi$. (Since we shall not have occasion to use a non-zero $\mathbf{v}$ in what follows it is set to zero, implying an irrotational $\dot{\mathbf{x}}$.)

Equation (8) may now be written as a weak form of an elliptic equation for ϕ

$$-\int_{\Omega(t)}w_i\nabla\cdot(\tilde{m}\nabla\phi)\,\mathrm{d}\Omega=\int_{\Omega(t)}w_i\left(\frac{\partial\tilde{m}}{\partial t}+\left(\frac{\partial\tilde{m}}{\partial u}+\frac{\partial\tilde{m}}{\partial\nabla u}\cdot\nabla\right)Lu\right)\mathrm{d}\Omega \tag{9}$$

A convenient weak form of the equations connecting $\dot{\mathbf{x}}$ and ϕ is

$$\int_{\Omega(t)}w_i(\dot{\mathbf{x}}-\nabla\phi)_k\,\mathrm{d}\Omega=0\quad\text{for } k=1,\ldots,d \tag{10}$$

We refer to (9) and (10) as the potential and velocity equations, respectively.

1.4. Finite elements

Following Reference [3], let $\mathbf{x}\approx\mathbf{X}$, a piecewise linear finite element mapping from some reference domain (typically $\Omega(1)$). This defines a moving finite element mesh on which $w_i\approx W_i$, the usual piecewise linear basis function at node i, whilst $\phi\approx\Phi$ and $u\approx U$ are piecewise linear approximations. The conservation principle (6) then becomes

$$\int_{\Omega(t)}W_i\tilde{m}(t,U,\nabla U)\,\mathrm{d}\Omega=C_i \tag{11}$$

say, where the C_i are known from the initial mesh and data. Similarly, the potential equation (9) may be expressed as

$$\int_{\Omega(t)} \tilde{m}\nabla W_i \cdot \nabla\Phi \,\mathrm{d}\Omega = \int_{\Omega(t)} W_i \left(\frac{\partial \tilde{m}}{\partial t} + \left(\frac{\partial \tilde{m}}{\partial U} + \frac{\partial \tilde{m}}{\partial \nabla U} \cdot \nabla \right) LU \right) \mathrm{d}\Omega \tag{12}$$

where $\Phi = 0$ has been applied on the boundary (corresponding to a zero tangential mesh velocity at the boundary). The velocity equation, (10), becomes

$$\int_{\Omega(t)} W_i(\dot{\mathbf{X}} - \nabla\Phi)_k \,\mathrm{d}\Omega = 0 \quad \text{for } k = 1, \ldots, d \tag{13}$$

corresponding to the best approximation $\dot{\mathbf{X}}$ to $\nabla\Phi$ in the space spanned by the W_i.

Using the finite element expansions $\mathbf{X} = \sum_j \mathbf{X}_j W_j, \Phi = \sum_j \Phi_j W_j, U = \sum_j U_j W_j$, the matrix forms of Equations (12) and (13) can be derived. These equations form the basis of the method whereby, given U on a mesh $\mathbf{X}$, a mesh velocity $\dot{\mathbf{X}}$ can be found. This is used to update the mesh via forward Euler time-stepping (say), after which the solution can be recovered on the new mesh via the conservation principle (11). Alternatively, U may also be approximated using time-stepping based upon the weak form

$$\int_{\Omega(t)} W_i \dot{U} \,\mathrm{d}\Omega = \int_{\Omega(t)} W_i(\nabla U \cdot \dot{\mathbf{X}} + LU) \,\mathrm{d}\Omega \tag{14}$$

with $\dot{U} = 0$ on the boundary of $\Omega(t)$.

2. MONITOR FUNCTIONS

The consequences of taking m to be the 'density' monitor function u have been extensively studied in Reference [3]. Many other choices for m are, however, possible. For the remainder of this paper we consider just one of these, the 'arc-length' monitor (widely used because of its tendency to move nodes into regions where the solution gradient is high) given by $\sqrt{1 + (\nabla u)^2}$, although the generalization to other monitors follows in a similar manner. From (7) $\tilde{m} = t^{-d\beta}\sqrt{1 + t^{2(\beta-\gamma)}(\nabla u)^2}$ and Equation (12) then becomes

$$\begin{aligned} &\int_{\Omega(t)} \sqrt{t^{-2(\beta-\gamma)} + (\nabla U)^2}\nabla W_i \cdot \nabla\Phi \,\mathrm{d}\Omega \\ &\quad = \int_{\Omega(t)} \frac{W_i}{t}(-d\beta + (\beta - \gamma))\sqrt{t^{-2(\beta-\gamma)} + (\nabla U)^2} \,\mathrm{d}\Omega \\ &\qquad + \int_{\Omega(t)} W_i \frac{-(\beta-\gamma)t^{-2(\beta-\gamma)-1} + \nabla U \cdot \nabla(LU)}{\sqrt{t^{-2(\beta-\gamma)} + (\nabla U)^2}} \,\mathrm{d}\Omega \end{aligned} \tag{15}$$

while (11) becomes

$$\int_{\Omega(t)} W_i t^{-d\beta}\sqrt{1 + t^{2(\beta-\gamma)}(\nabla U)^2} \,\mathrm{d}\Omega = C_i \tag{16}$$

3. APPLICATIONS

3.1. The porous medium equation (PME)

Using the values of β and γ noted in Section 1 with the arc-length monitor, (15) gives

$$\int_{\Omega(t)} \sqrt{t^{-2(d+1)/(nd+2)} + (\nabla U)^2}\, \nabla W_i \cdot \nabla \Phi \, \mathrm{d}\Omega$$

$$= \int_{\Omega(t)} \frac{W_i t^{-1}}{nd+2} \sqrt{t^{-2(d+1)/(nd+2)} + (\nabla U)^2}\, \mathrm{d}\Omega$$

$$+ \int_{\Omega(t)} W_i \frac{-(d+1)t^{-((n+2)d+4)/(nd+2)}/(nd+2) + \nabla U \cdot \nabla Q}{\sqrt{t^{-2(d+1)/(nd+2)} + (\nabla U)^2}}\, \mathrm{d}\Omega \tag{17}$$

while (16) becomes

$$\int_{\Omega(t)} W_i t^{-d/(nd+2)} \sqrt{1 + t^{2(d+1)/(nd+2)} (\nabla U)^2}\, \mathrm{d}\Omega = C_i \tag{18}$$

Note that due to the piecewise linear approximation it is necessary to introduce an intermediate finite element function $Q \approx LU$ in (17), recovered from the weak form

$$\int_{\Omega(t)} W_i Q \, \mathrm{d}\Omega = -\int_{\Omega(t)} U^n \nabla W_i \cdot \nabla U \, \mathrm{d}\Omega \tag{19}$$

Results for the one-dimensional equation are shown in Figure 1. In each case the results shown were obtained using (14) to update the values of the dependent variable and the initial mesh was uniformly spaced. The test case shown models a similarity solution to the PME of the form given in Reference [3, 6]. When $n = 1$ the scheme exhibits close to second-order accuracy, while when $n = 2$ (and higher) the exact solution has infinite gradient at the boundary and the numerical order of accuracy reduces to approximately one.

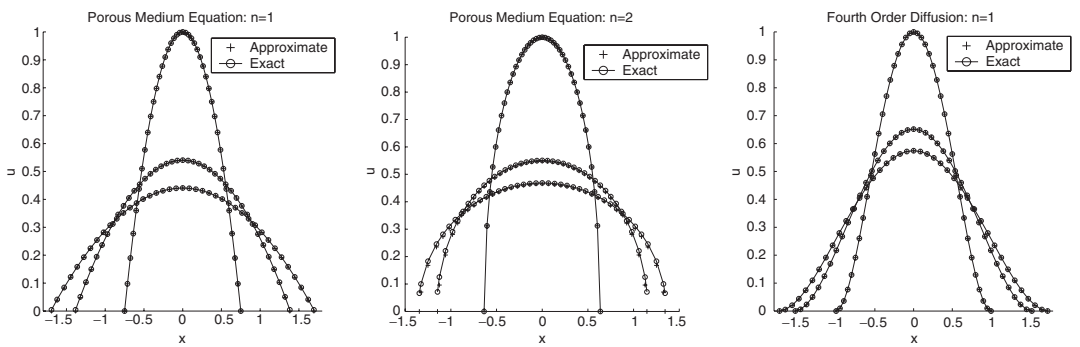

Figure 1. Snapshots of one-dimensional results at various times illustrating: PME with $n = 1$ (left); PME with $n = 2$ (middle); 4th order with $n = 1$ (right).

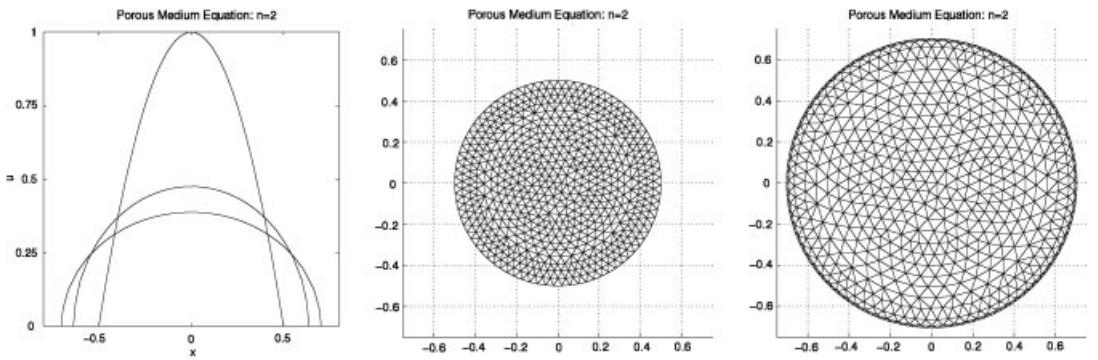

Figure 2. Snapshots of two-dimensional results at various times illustrating the evolution of the PME solution with $n=2$ from initial conditions that do not correspond to a similarity solution: successive slices through $y=0$ (left); initial mesh (middle); final mesh (right).

Similar results are seen in two dimensions when comparisons are made with exact similarity solutions. However, Figure 2 does not show a similarity solution, instead it has been chosen to illustrate the movement of the mesh towards a region (the moving boundary in this case) in which the gradient of the evolving solution is steepening. The conservation of arc-length can clearly be seen to lead to a reduction in the mesh size in the regions where the gradient has increased sharply over time.

3.2. *A fourth-order equation*

In order to apply the proposed algorithm to the fourth-order problem (4) using piecewise linear finite elements it is necessary to express it as a pair of second-order equations:

$$u_t + \nabla \cdot (u^n \nabla p) = 0, \quad p = \nabla^2 u \tag{20}$$

As with the PME, appropriate values of β and γ (see Section 1) may be substituted into (15) in order to obtain equations for the mesh potential function Φ. Again it is necessary to replace LU by a weak approximation, Q, in this case given by

$$\int_{\Omega(t)} W_i Q \, \mathrm{d}\Omega = -\int_{\Omega(t)} U^n \nabla W_i \cdot \nabla P \, \mathrm{d}\Omega \tag{21}$$

where P is the finite element approximation to p given by

$$\int_{\Omega(t)} W_i P \, \mathrm{d}\Omega = -\int_{\Omega(t)} \nabla W_i \cdot \nabla U \, \mathrm{d}\Omega \tag{22}$$

Figure 1 shows one set of results for this fourth-order equation and compares them with the exact similarity solution given in References [3, 5] when $n=1$. The numerical results suggest an order of accuracy of between 1 and 2 in one dimension and approximately 1 in two dimensions.

4. DISCUSSION

We have presented a moving mesh finite element method based on the use of a scale invariant conservation principle incorporating an arc length monitor function. Symmetric computational results have been included, simply to illustrate typical behaviour and performance for this method, but scale invariance does not depend on symmetry [4] and the technique is far more generally applicable [3]. There is no reason why it cannot be applied much more widely, to more complicated geometries with other monitors and other problems exhibiting scale invariance.

REFERENCES

1. Budd CJ, Piggott M. The geometric integration of scale-invariant ordinary and partial differential equations. *Journal of Computational and Applied Mathematics* 2001; **128**:399–422.
2. Cao W, Huang W, Russell RD. A moving mesh method based on the geometric conservation law. *SIAM Journal on Scientific Computing* 2002; **24**:118–142.
3. Baines MJ, Hubbard ME, Jimack PK. A moving mesh finite element algorithm for the adaptive solution of time-dependent partial differential equations with moving boundaries. *Applied Numerical Mathematics* 2004, in press.
4. Barenblatt GI. *Scale Invariance*, *Self-similarity and Intermediate Asymptotics*. Cambridge University Press: Cambridge, 1996.
5. Diez JA, Kondic L, Bertozzi A. Global models for moving contact lines. *Physics Review E* 2001; **63**:011208.
6. Murray JD. *Mathematical Biology*: *An Introduction* (3rd edn). Springer: Berlin, 2002.

